Electron Spin-Echo Studies of the Copper(II) Binding Sites in Dopamine β-Hydroxylase†

John McCracken,*,‡ Parimal R. Desai,§ Nicholas J. Papadopoulos,§ Joseph J. Villafranca,§ and Jack Peisach‡

Departments of Molecular Pharmacology and Physiology and Biophysics, Albert Einstein College of Medicine of Yeshiva University, Bronx, New York 10461, and Department of Chemistry, The Pennsylvania State University, University Park, Pennsylvania 16802

Received December 8, 1987

ABSTRACT: The active site structure of Cu(II) in dopamine β-hydroxylase, isolated from bovine adrenal medulla, was studied by pulsed electron paramagnetic resonance (EPR) spectroscopy. Fourier transformation of the stimulated electron spin-echo envelope revealed frequency components characteristic of Cu(II)–histidyl imidazole coordination. The three major lines in the spectrum at 0.7, 1.4, and 4.0 MHz are typical for Cu(II)–imidazole complexes where imidazole is protonated and equatorially coordinated. Quantitation of the number of imidazole ligands bound to Cu(II) in enzyme containing two, four, and eight Cu per protein tetramer, as well as characterization of the superhyperfine coupling parameters, was achieved by spectral simulation. In all cases, it was shown that there are three, or more likely four, imidazole ligands bound to Cu(II). Addition of deuteriated substrate analogues to the enzyme did not produce any observable deuterium modulation in the spin-echo envelopes, thus indicating that the distance between substrate deuterons and Cu(II) is greater than 5 Å.

Dopamine β-hydroxylase (EC 1.14.17.1), found within vesicles of the adrenal medulla and noradrenergic nerve cells, catalyzes the conversion of dopamine to norepinephrine. The enzyme, in both membrane-bound and soluble forms, is a tetrameric, copper-containing glycoprotein monoxygenase (Kaufman & Friedman, 1965; Skotland & Ljones, 1979; Rosenberg & Lovenberg, 1980; Villafranca, 1981). When isolated, the copper content of this protein is variable, ranging from two to ten copper atoms per tetramer (Blackburn et al., 1980; Skotland & Ljones, 1983). However, it has only been recently shown that fully active enzyme contains approximately eight copper atoms per tetramer (Ash et al., 1984; Colombo et al., 1984; Klinman et al., 1984). As enzyme-bound copper, as Cu(II), is reduced by ascorbate (Blumberg et al., 1965; Friedman & Kaufman, 1966; Walker et al., 1977), it is thought to play a role in the catalytic cycle.

The nature of the Cu(II) binding site in DβH[1] has previously been studied by continuous-wave EPR spectroscopy (Blumberg et al., 1965; Friedman & Kaufman, 1966; Walker et al., 1977; Ljones et al., 1978; Skotland et al., 1980; Villafranca et al., 1982). It was shown that DβH is typical of type 2 copper proteins (nonblue, EPR detectable) with bound Cu(II) magnetically noninteracting. Cysteine sulfur ligation to Cu(II) is ruled out, as the intense color and a characteristic EPR spectrum of type 1 Cu(II) centers are not seen. The spin Hamiltonian parameters obtained by EPR (Papadopoulos, 1985) for fully active DβH containing eight Cu(II)/tetramer ($g_\perp = 2.07$ $g_\parallel = 2.27$, and $A_\parallel = 0.0150$ cm^{-1}) are consistent with tetragonal coordination of four nitrogen or mixed nitrogen/oxygen equatorial metal ligation (Peisach & Blumberg, 1974). However, EPR measurements do not readily distinguish between different types of copper binding sites in this protein (Skotland et al., 1980) or whether all copper atoms are identical with respect to their ligands and symmetries. In addition, EPR studies do not address the problem of the relative proximities to Cu(II) of substrates and the anion activator fumarate (Friedman & Kaufman, 1966). Since a knowledge of the nature and geometry of the ligands at the metal center is important for eventually understanding the reactivity of the metal ion, we have undertaken pulsed EPR studies to determine metal ligand identity. In the current investigation, we have used the electron spin-echo envelope modulation (ESEEM) technique (Kevan, 1979; Mims & Peisach, 1981) to characterize the magnetic interactions between Cu(II) and weakly coupled magnetic nuclei in DβH and in this way to identify and define the structure of the metal binding site(s).

Experimental Procedures

Materials. Chemicals and buffers were from Sigma Chemical Co. unless otherwise noted. D_2O and the deuteriated substrates of DβH, 2-(4-hydroxyphenyl)[1,1-$^2H_2$]ethylamine, and 2-(4-hydroxyphenyl)[2,2-$^2H_2$]ethylamine, were purchased from MSD Isotopes. Concanavalin A–Sepharose was from Pharmacia, (diethylaminoethyl)cellulose (DE-53) was from Whatman, and catalase (crystalline suspension in water, 65000 units/mg) was from Boehringer. CENTRICON-10 microconcentrators, used for small-volume protein concentration, were purchased from Amicon.

DβH was purified from bovine adrenal medulla. Enzyme activity was followed by monitoring oxygen consumption polarographically with a Clark oxygen electrode at pH 5.0 and 37 °C (Colombo et al., 1987). Protein concentration was determined spectrophotometrically at 280 nm with the ex-

† This work was supported by NIH Grants GM 29139 (J.J.V.) and RR 02583 and HL 13399 (J.P.).

* Correspondence should be addressed to this author.
‡ Albert Einstein College of Medicine of Yeshiva University.
§ The Pennsylvania State University.

[1] Abbreviations: DβH, dopamine β-hydroxylase; dien, diethylenetriamine; EPR, electron paramagnetic resonance; ESE, electron spin echo; ESEEM, electron spin-echo envelope modulation; G, gauss; Mes, 2-(*N*-morpholino)ethanesulfonic acid; nqi, nuclear quadrupole interaction; shf, superhyperfine; NQR, nuclear quadrupole resonance; PAS, principle axis system.

0006-2960/88/0427-4133$01.50/0

tinction coefficient $\epsilon^{1\%} = 12.4$ (Skotland & Ljones, 1977). A tetramer molecular mass of 290 000 Da (Wallace et al., 1973) was used in the calculations of enzyme concentration and copper content.

Copper was determined by atomic absorption with a Perkin-Elmer 3030 flameless atomic absorption spectrometer equipped with an HGA 500 graphite furnace programmer, by monitoring the absorption at 324.8 nm. Copper standards, from Scientific Products, were made 0.78 μM (0.050 ppm), 1.57 μM (0.100 ppm), and 2.36 μM (0.150 ppm) in Cu. The standard addition method was employed to calculate the copper content of DβH samples which were diluted 350-fold so that the final concentrations were in the linear working range of the standard curve.

The purified enzyme (stored as a suspension in ammonium sulfate), when dialyzed against 50 mM Mes, pH 5.5, invariably contained about two Cu per DβH tetramer (1.9–2.4). Protein containing eight Cu per tetramer (7.7–8.5) was prepared by dialysis of the two Cu per tetramer enzyme against 50 mM Mes, pH 5.5, containing 10 μM $CuCl_2$, then containing 1 μM $CuCl_2$, and finally containing no added $CuCl_2$. The three buffer changes were made over a 24-h period with a 250-fold volume each of excess dialyzing solution. The preparation of a ~4 Cu/tetramer sample required dialyzing against 50 mM Mes, pH 5.5, containing 6 μM $CuCl_2$ for the first change and no added $CuCl_2$ for the last two changes. This resulted in about 3.7–3.9 mol of Cu/mol of tetramer. The copper concentration of various DβH samples used for ESEEM measurements ranged from 0.2 to 1.5 mM.

The pulsed EPR spectrometer used in these studies has been described in detail elsewhere (McCracken et al., 1987). Two different microwave cavity systems were used for ESEEM measurements. For dilute ([Cu(II)] < 0.5 mM) enzyme samples, a stripline transmission cavity, identical with the one developed by Mims, was utilized (Mims, 1974). For preparations more concentrated in Cu(II), a reflection cavity system (Britt & Klein, 1987) that employs a folded stripline as the resonant element was used (Lin et al., 1985). The ESEEM data presented below were collected with the stimulated echo pulse sequence (90°–τ–90°–T–90°) (Hahn, 1950) with τ values set so that modulations due to weakly coupled protons were suppressed (Mims & Peisach, 1981). Fourier transformation of the time domain data was achieved with a modified version of the dead time reconstruction technique of Mims (1984).

Results and Discussion

A stimulated echo ESEEM pattern for DβH containing eight Cu per tetramer, together with the ESEEM spectrum obtained by Fourier transformation, is shown in Figure 1. Identical results with those of Figure 1 were obtained for DβH containing either two or four Cu per tetramer (for direct comparison, the samples contained approximately the same amount of total copper). Four frequency components are clearly resolved in the Fourier transform: two narrow lines at 0.7 and 1.4 MHz, a broad component centered at 4.0 MHz, and a minor component at 2.1 MHz. The spectrum of Figure 1 is nearly identical with those obtained for Cu(II)–imidazole model complexes (Mims & Peisach, 1978) and for several Cu(II) proteins (Mondovi et al., 1977; Mims & Peisach, 1979; Kosman et al., 1980; Avigliano et al., 1981) and arises from magnetic coupling between Cu(II) and the remote ^{14}N of equatorially bound imidazole (Mims & Peisach, 1978). The narrow, low-frequency components at 0.7 and 1.4 MHz arise from that ^{14}N superhyperfine spin manifold where nuclear Zeeman and electron nuclear hyperfine interaction approximately cancel one another, so that the energy level splittings are primarily determined by the ^{14}N nuclear quadrupole interaction. The other shf spin manifold gives rise to much broader resonances with the only resolvable component occurring at approximately 4 MHz.

The ESEEM spectrum of DβH also shows minor frequency components at 2.1 and 2.9 MHz.[2] These are attributable to "combination" frequencies, and are observed when more than a single imidazole ligand is magnetically coupled to protein Cu(II) (Kosman et al., 1980; McCracken et al., 1988). They are a consequence of the product rule for ESEEM (Rowan et al., 1965; Mims, 1972; Dikanov et al., 1977), and their relative amplitudes as compared to those of the 0.7- and 1.4-MHz lines in the ESEEM spectrum provide information concerning the number of imidazoles equatorially coordinated to Cu(II) (McCracken et al., 1988).

A notable point concerning the frequency spectrum shown in Figure 1 is that the line shape of the ~4-MHz component differs significantly from that found for the model compounds Cu^{II}(dien)(imid) (Figure 2) and $Cu^{II}(imid)_4$. For the protein (Figure 1) there appears to be two peaks, one at 3.8 MHz and a second at 4.1 MHz, whereas for the model (Figure 2B), only one is seen. This complex line shape might reflect two magnetically distinct populations of bound histidyl residues, one with a slightly larger electron–nuclear hyperfine coupling than the other, or alternatively it might be a consequence of the relative orientations of the principle axis systems of the electron–nuclear hyperfine and nqi tensors (Reijerse & Keijzers, 1987). Both of these possibilities are considered.

A detailed analysis based on computer simulations of the ESEEM for DβH was carried out to better characterize the magnetic coupling between Cu(II) and histidyl imidazole and to quantify the number of such ligands bound. This analysis utilizes the density matrix formalism of Mims (Mims, 1972; Reijerse & Keijzers, 1987) and has been described in detail elsewhere (McCracken et al., 1987; Magliozzo et al., 1987). A useful starting point for the analysis is the ESEEM of Cu^{II}(dien)(imid). As the principle frequency components for this model complex closely match those for the enzyme, analysis of model complex data provides information concerning the principle elements of the hyperfine coupling tensor, the nqi tensor, and the relationship between their principle axis systems. ESEEM data and the associated Fourier transform for Cu^{II}(dien)(imid) are shown in Figure 2 (solid line) along with a simulation of the time domain data (dashed line). To a first approximation, the frequency spectrum is similar to that of DβH, showing a broad line at 0.7 MHz, a narrower component at 1.4 MHz, and a broad line at 4.0 MHz. The difference between the ESEEM data of Figures 1 and 2 is that no combination lines are observed at 2.1 and 2.9 MHz in the latter, since only a single imidazole is coordinated to Cu(II) in the model complex. Also, the broad peak at 0.7 MHz seen for the protein is clearly resolved into two narrow lines at 0.6 and 0.8 MHz for Cu^{II}(dien)(imid), and the 4.0-MHz component for the model complex has an asymmetric line shape with a single peak skewed toward higher frequency.

The spin Hamiltonian parameters used for the simulation of the ^{14}N ESEEM of Cu^{II}(dien)(imid), along with other details of the calculation, are given in the caption for Figure 2. An axial hyperfine tensor was used with a best fit value of the Fermi contact term of 1.6 MHz. The Euler angles

[2] The 2.9-MHz component was better resolved for stimulated echo modulation data taken at τ values other than that used for Figure 1 (data not shown).

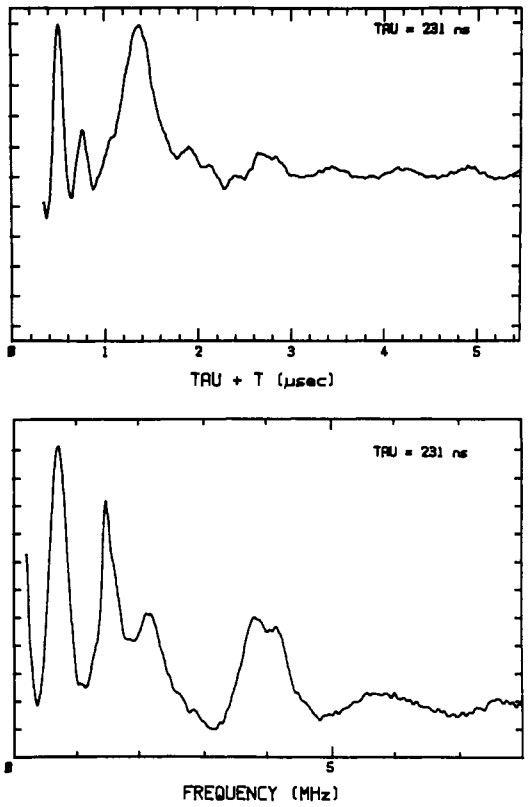

FIGURE 1: Stimulated ESEEM data and associated Fourier transform for dopamine β-hydroxylase containing eight Cu per tetramer. Experimental conditions were as follows: microwave frequency, 8.75 GHz; magnetic field strength, 3050 G; microwave pulse power, 40 W (20-ns full-width half-maximum); sample temperature, 4.2 K; τ value, 231 ns. Fifty events were averaged at each time point with a pulse sequence repetition rate of 100 Hz. The Cu(II) concentration for this sample was 1.1 mM.

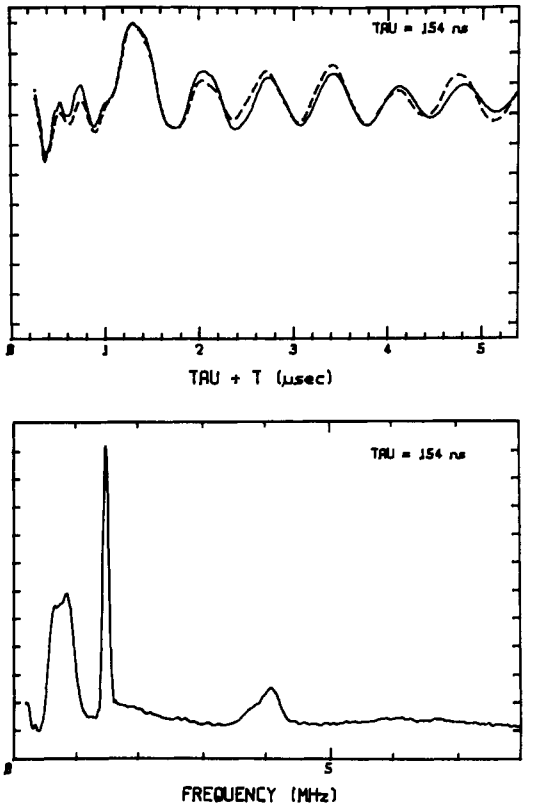

FIGURE 2: Stimulated ESEEM data (solid line) and associated Fourier transform for the Cu^{II}(dien)(imid) model complex. Experimental conditions were identical with those given in Figure 1 except that a τ value of 154 ns was utilized. The dashed curve, in the upper panel, displayed along with the time domain data, shown by the solid line, represents a computer simulation of data with the following spin Hamiltonian parameters: A_{xx}, A_{yy}, 1.45 MHz; A_{zz}, 2.0 MHz; e_2qQ, 1.5 MHz; η, 0.82; Euler angles, $\alpha = \gamma = 0°$, $\beta = 90°$; g_n, 0.40349. To facilitate comparison with data, the simulation was multiplied by an exponential decay function, $\exp[(t/\tau)^{0.5}]$, where $\tau = 7.0$ μs.

describing the relative orientation of the nqi tensor with respect to the hyperfine tensor were $\alpha = 0°$, $\beta = 90°$, and $\gamma = 0°$.[3] Using this set of Euler angles to describe the relative orientation between hyperfine and nqi tensors for Dβ H, we found that simulation of the "double-peaked" line shape of the 4-MHz component for the protein sample (Figure 1) required that two magnetically distinct populations of bound imidazole residues be considered. The spin Hamiltonian parameters used for these two sets of coupled ^{14}N nuclei differed only in the magnitude of their Fermi contact interactions with Cu(II), the anisotopic portion of the hyperfine tensor and the nqi parameters being identical. The simulations obtained with this approach are shown in Figure 3A along with ESEEM data (solid line) collected for Dβ H containing eight Cu(II) per enzyme tetramer. The dashed line is a simulated ESEEM arising from four magnetically coupled nitrogens,[4] two with a Fermi contact of 1.8 MHz and two with a contact interaction of 1.3 MHz. Both hyperfine tensors were taken as axial with a dipolar contribution similar to that found for Cu^{II}(dien)-(imid). The nqi parameters used for both sets of nuclei were $e^2qQ = 1.44$ MHz and $\eta = 0.90$, nearly identical with the values determined by NQR studies on imidazole powders (Hunt et al., 1975). For simulations that considered three magnetically coupled nitrogens, it was necessary to include a third magnetically distinct nucleus in the calculation, with a Fermi contact term of 1.55 MHz, to account for the line shape of the 4-MHz component in the Dβ H data. The result is shown as the dash–dot pattern in Figure 3A. With only two imidazoles, one of each type used in the four-imidazole simulation, the modulations are far too weak to explain the data, and these are shown as the dotted line of Figure 3A.

At first glance, then, the results of Figure 3A would lead one to conclude that four histidyl imidazole ligands are equatorially bound to Cu(II) in Dβ H. This conclusion is in agreement with results of previous EXAFS studies (Hasnain et al., 1984). However, because the experimentally determined ESEEM represents the product of the modulations due to each contributing nucleus with a background decay function (Kevan, 1979), some uncertainty exists in comparing modulation depths or amplitudes obtained experimentally with those calculated from first principles. To facilitate comparison of experiment and theory, the calculated ESEEM functions of Figure 3A were multiplied by an exponential decay function of the form $\exp[-(t/\tau)^{0.5}]$, where the base line for the decay was chosen to coincide with that obtained experimentally. For Dβ H, a decay time constant (τ) of 350 ns was needed to give the initial peak in the modulation pattern (at 0.5 μs) approximately the same amplitude as the peak at about 1.35 μs. Because this decay function was found to be so rapid for the protein, the uncertainty in comparing experiment and theory is great enough that one cannot say with confidence that the ESEEM for Dβ H arises from four histidyl imidazoles equa-

[3] Euler angle rotation as defined in Silver (1976).

[4] Computer simulations of ESEEM interactions arising from multiple nuclei make use of the spherical model approximation to the product rule (Kevan et al., 1975). The consequences of using this approximation for the weak ^{14}N magnetic couplings encountered for Cu(II)–imidazole model compounds and Cu(II) proteins have been addressed elsewhere (McCracken et al., 1988).

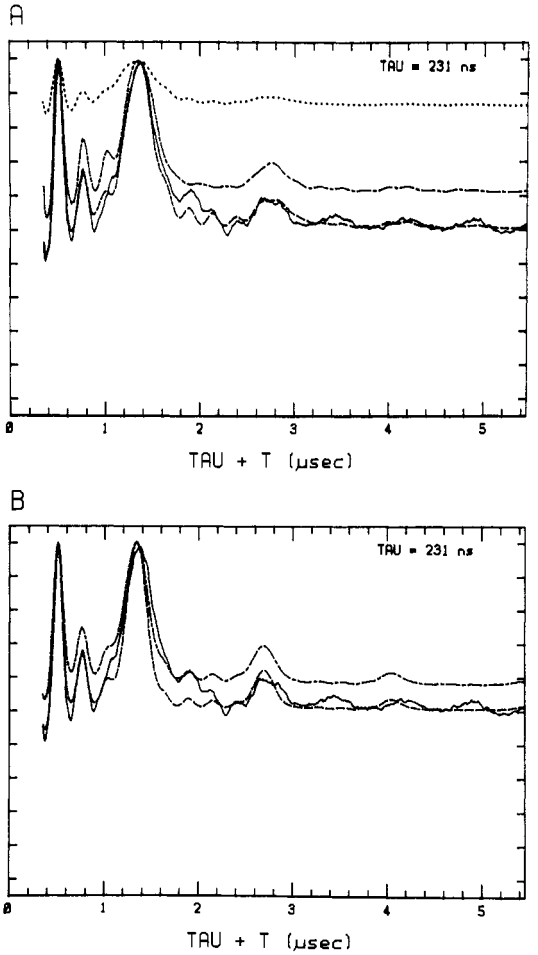

FIGURE 3: A comparison of the stimulated ESEEM data obtained for dopamine β-hydroxylase containing eight Cu per tetramer (solid line) with computer simulations of ESEEM for Cu^{II}(imid) models containing four magnetically coupled ^{14}N nuclei (– –), three coupled ^{14}N (–·–), and two coupled ^{14}N (···). For (A), a model that considered different populations of magnetically distinct ^{14}N nuclei was used; while for (B), only a single set of magnetic coupling parameters was considered. For (A), the spin Hamiltonian parameters used were as follows: $(A_{xx}, A_{yy}, A_{zz})_{\text{nucleus 1}}$, (1.1, 1.1, 1.7 MHz); $(A_{xx}, A_{yy}, A_{zz})_{\text{nucleus 2}}$, (1.6, 1.6, 2.2 MHz); e^2qQ, 1.44 MHz; η, 0.90; (α, β, γ), (0°, 90°, 0°); g_n 0.40349. The two-^{14}N simulation for two coordinated imidazoles (dotted line) consisted of contributions from one weakly coupled ^{14}N (nucleus 1) and one strongly coupled ^{14}N (nucleus 2), while the four-^{14}N simulation (dashed line) consisted of contributions from a pair of each type of nucleus. The three-^{14}N simulation of (A) (dot–dash pattern) considered contributions from one each of the two nuclei described above and a third ^{14}N with $A_{xx} = A_{yy} = 1.35$ MHz and $A_{zz} = 1.95$ MHz. The spin Hamiltonian parameters used for (B) were as follows: (A_{xx}, A_{yy}, A_{zz}), (1.5, 1.5, 2.25 MHz); e^2qQ, 1.44 MHz; η, 0.98; (α, β, γ), (0°, 32°, 0°).

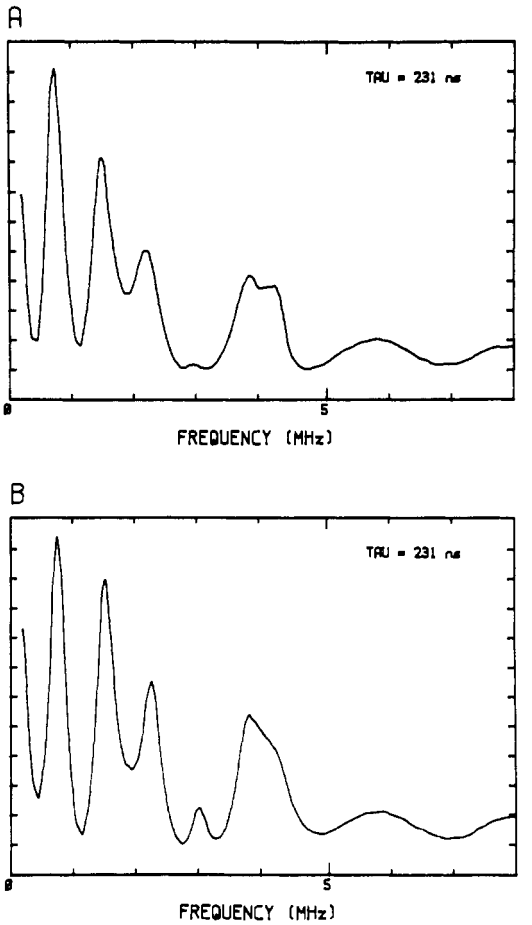

FIGURE 4: Fourier transforms of the ^{14}N simulations for four imidazoles coordinated to Cu(II) from Figure 3A,B displayed in (A) and (B), respectively. In (A), two sets of ^{14}N nuclei with different coupling parameters are considered while in (B) a four-imidazole model with identical coupling but with differing orientations of hyperfine and nqi parameters is considered.

torially bound to Cu(II), and one must consider that possibly the three are coordinated.

An alternative analysis is suggested by the complex line shape of the 4.0-MHz component in the ESEEM spectrum of DβH (Figure 1), which may be a consequence of the relative orientations of the hyperfine and nqi coupling tensors (Reijerse & Keijzers, 1987) for a single set of magnetic coupling parameters. ESEEM simulations using this approach are shown in Figure 3B along with the experimental data (solid line). As with the previous model, the four-nitrogen simulation (dashed curve) appears to account for the modulation depth better than the three-nitrogen model (dash–dot pattern). However, for the reasons given above, a choice between three or four bound histidyl imidazoles cannot be made with certainty.

The Fourier transforms of the four-nitrogen simulations for the two models presented in panels A and B of Figure 3 are shown in panels A and B of Figure 4, respectively. Both models predict with accuracy the frequencies, relative amplitudes, and damping factors of the 0.7, 1.4, and 4.0-MHz components of the spectrum. However, the combination lines observed for the single parameter set simulation (Figure 4B) are sharp and well resolved. This is in contrast to the experimental data (Figure 1) and the Fourier transform of the simulations due to two magnetically distinct pairs of coupled ^{14}N nuclei (Figure 4A), where a broad component was observed at 2.1 MHz, and the 2.9-MHz component was not clearly resolved. Because several approximations are made in the theoretical treatment used to obtain the simulations of Figure 3, further speculation concerning the relative merits of these two models is not warranted at this time. For either case, however, four-imidazole coordination to Cu(II) in DβH containing either two, four, or eight Cu/tetramer is demonstrated, although there is sufficient uncertainty that one cannot rule out three-imidazole coordination. In favor of three-imidazole coordination is a recent ^1H NMR relaxation study of DβH treated with either cyanide or azide which provides indirect evidence for a single water equatorially coordinated to Cu(II), with a second water axially bound (Obata et al., 1987). However, as the authors state, equivocal conclusions concerning the untreated protein cannot be derived from this work as structural rearrangement of ligands may be brought about by anion binding.

In addition to ESEEM studies on resting enzyme, DβH samples with eight Cu/tetramer were treated with two dif-

ferent substrate analogues, [1,1-$^2H_2$]tyramine (20 mM) and [2,2-$^2H_2$]tyramine (20 mM), and these were examined in order to determine the distance between Cu(II) and a close deuteron on a bound substrate analogue, either in the presence or absence of fumarate (10 mM) (Goldstein et al., 1968). Deuterium ESEEM was not observed for any of the four samples studied, suggesting that deuterons on a substrate analogue are at least 4.5–5.0 Å from Cu(II), provided that each Cu(II) of the protein interacts with substrate. If only a few metal atoms of the eight Cu(II) per tetramer protein are at sites where substrate is bound, then the ability to detect deuteron modulations, already reduced because of deep ^{14}N ESEEM, would be reduced still further, thus providing an alternative explanation for the absence of deuterium modulation for these enzyme complexes.

Recent kinetic studies with DβH inhibitors (Kruse et al., 1986) suggest an ordered addition of substrate to enzyme for catalysis, with preferential substrate binding to reduced enzyme. Were substrate to bind poorly to oxidized EPR-active protein, then deuterium modulation from deuteriated substrates would not be expected.

Registry No. DβH, 9013-38-1; Cu, 7440-50-8; L-histidine, 71-00-1.

REFERENCES

Ash, D. E., Papadopoulos, N. P., Colombo, G., & Villafranca, J. J. (1984) *J. Biol. Chem. 259*, 3395–3398.

Avigliano, L., Davis, J. L., Graziani, M. T., Marchesini, A., Mims, W. B., Mondovi, B., & Peisach, J. (1981) *FEBS Lett. 136*, 80–84.

Blackburn, N. J., Mason, H. S., & Knowles, P. F. (1980) *Biochem. Biophys. Res. Commun. 95*, 1275–1281.

Blumberg, W. E., Goldstein, M., Lauber, E., & Peisach, J. (1965) *Biochim. Biophys. Acta 99*, 187–190.

Britt, R. D., & Klein, M. P. (1987) *J. Magn. Reson. 74*, 535–540.

Colombo, G., Rajashekhar, B., Giedroc, D. P., & Villafranca, J. J. (1984) *Biochemistry 23*, 3590–3598.

Colombo, G., Papadopolous, N. J., Ash, D. E., & Villafranca, J. J. (1987) *Arch. Biochem. Biophys. 252*, 71–80.

Dikanov, S. A., Yudanov, V. F., & Tsvetkov, Yu. D. (1977) *J. Struct. Chem. 18*, 460–476.

Friedman, S., & Kaufman, S. (1966) *J. Biol. Chem. 241*, 2256–2259.

Goldstein, M., Joh, T. H., & Garvey, T. Q. (1968) *Biochemistry 7*, 2724–2730.

Hahn, E. L. (1950) *Phys. Rev. 80*, 580–594.

Hasnain, S. S., Diakun, G. P., Knowles, P. F., Binsted, N., Garner, C. D., & Blackburn, N. J. (1984) *Biochem. J. 221*, 545–548.

Hunt, M. J., Mackay, A. L., & Edmonds, D. T. (1975) *Chem. Phys. Lett. 34*, 473–475.

Kaufman, S., & Friedman, S. (1965) *Pharmacol. Rev. 17*, 71–100.

Kevan, L. (1979) in *Time Domain Electron Spin Resonance* (Kevan, L., & Schwartz, R. N., Eds.) pp 279–342, Wiley-Interscience, New York.

Kevan, L., Bowman, M. K., Narayana, D. A., Boeckman, R. K., Yudanov, V. F., & Tsvetkov, Yu. D. (1975) *J. Chem. Phys. 63*, 409–416.

Klinman, J. P., Krueger, M., Brenner, M., & Edmonson, D. E. (1984) *J. Biol. Chem. 259*, 3399–3402.

Kosman, D. J., Peisach, J., & Mims, W. B. (1980) *Biochemistry 19*, 1304–1308.

Kruse, L. I., DeWolf, W. E., Chambers, P. A., & Goodhart, P. J. (1986) *Biochemistry 25*, 7271–7278.

Lin, C. P., Bowman M. K., & Norris, J. R. (1985) *J. Magn. Reson. 65*, 369–374.

Ljones, T., Flatmark, T., Skotland, T., Peterson, L., Backstrom, D., & Ehrenberg, A. (1978) *FEBS Lett 92*, 81–84.

Magliozzo, R. S., McCracken, J., & Peisach, J. (1987) *Biochemistry 26*, 7923–7931.

McCracken, J., Peisach, J., & Dooley, D. M. (1987) *J. Am. Chem. Soc. 109*, 4064–4072.

McCracken, J., Pember, S. O., Benkovic, S. J., Villafranca, J. J., Miller, R. J., & Peisach, J. (1988) *J. Am. Chem. Soc. 110*, 1069–1074.

Mims, W. B. (1972) *Phys. Rev. B: Solid State 5*, 2409–2419.

Mims, W. B. (1974) *Rev. Sci. Instrum. 45*, 1583–1591.

Mims, W. B. (1984) *J. Magn. Reson. 59*, 291–306.

Mims, W. B., & Peisach, J. (1978) *J. Chem. Phys. 69*, 4921–4930.

Mims, W. B., & Peisach, J. (1979) *J. Biol. Chem. 254*, 4321–4323.

Mims, W. B., & Peisach, J. (1981) in *Biological Magnetic Resonance* (Berliner, L. J., & Reuben, J., Eds.) Vol. 3, pp 212–264, Plenum, New York.

Mondovi, B., Graziani, M. T., Mims, W. B., Oltzik, R., & Peisach, J. (1977) *Biochemistry 16*, 4198–4202.

Obata, A., Tanaka, H., & Kawazura, H. (1987) *Biochemistry 26*, 2962–2968.

Papadopoulos, N. J. (1985) Ph.D. Thesis, The Pennsylvania State University.

Peisach, J., & Blumberg, W. E. (1974) *Arch. Biochem. Biophys. 165*, 691–708.

Reijerse, E. J., & Keijzers, C. P. (1987) *J. Magn. Reson. 71*, 83–96.

Rosenberg, R. C., & Lovenberg, W. (1980) *Essays Neurochem. Neuropharmacol. 4*, 163–209.

Rowan, L. G., Hahn, E. L., & Mims, W. B. (1965) *Phys. Rev. [Sect.] A 137*, 61–71.

Silver, B. L. (1976) *Irreducible Tensor Methods*, pp 1–5, Academic, New York.

Skotland, T., & Ljones, T. (1977) *Int. J. Pept. Protein Res. 10*, 311–314.

Skotland, T., & Ljones, T. (1979) *Inorg. Perspect. Biol. Med. 2*, 151–180.

Skotland, T., & Ljones, T. (1983) *J. Inorg. Biochem. 18*, 11–18.

Skotland, T., Peterson, L., Backstrom, D., Ljones, T., Flatmark, T., & Ehrenberg, A. (1980) *Eur. J. Biochem. 103*, 5–11.

Villafranca, J. J. (1981) in *Copper Proteins* (Spiro, T. G., Ed.) pp 264–289, Wiley, New York.

Villafranca, J. J., Colombo, G., Rajashekhar, B., Giedroc, D., & Baldoni, J. (1982) in *Oxygenases and Oxygen Metabolism* (Nozaki, M., Yamamoto, S., Ishimura, Y., Coon, M. J., Ernster, L., & Estabrook, R. W., Eds.) pp 125–135, Academic, New York.

Walker, G. A., Kon, H., & Lovenberg, W. (1977) *Biochim. Biophys. Acta 482*, 309–327.

Wallace, E. F., Krantz, M. J., & Lovenberg, W. (1973) *Proc. Natl. Acad. Sci. U.S.A.* 70, 2253–2255.